Condition Monitoring of Large Oil and Chemical Storage Tanks Using Long Range Ultrasonic Testing (LRUT)

Davide Kleiner, Chris Edwards and Ruth Sanderson
TWI ltd.
Granta Park, Great Abington
Cambridge CB1 6AL
Tel. 01223 891162
e-mail: davide.kleiner@twi.co.uk
chris.edwards@twi.co.uk
ruth.sanderson@twi.co.uk

R.Kažys, V.Cicenas, R.Raišutis, E.Jasiuniene and K.Baršauskas
Ultrasound Institute
Kaunas University of Technology
Studentu 50
3031 Kaunas
Lithuania

SYNOPSIS

Large storage tanks containing hazardous liquids such as oil, oil-derived products and food processing liquids are common throughout the world. Corrosion in the tank floor is a serious environmental and economic risk.

TWI is managing a European CRAFT project called TANKINSPECT to overcome the drawbacks of current inspection practices. By placing Long Range Ultrasonics (LRUT) sensors outside the tank and using reconstructive tomographic techniques there is potential for carrying out an inspection of the whole tank floor without the requirement of emptying and cleaning the tank or operator entry inside the tank.

The project, a €2million Framework 6 project, started in March 2004 and is due to finish in February 2005. The research carried out so far has already shown very promising results both on the numerical modelling and the practical inspection development sides, making the consortium very confident that a working product will be successfully delivered by the end of the project.

1 INTRODUCTION

Numerical modelling of ultrasonic wave propagation has been carried out in structures representative of storage tank floors. The floors are constructed from overlapping lap welded steel plates. The attenuation of waves propagating in lap welded steel plates loaded by diesel and sitting on wet sand has previously been reported [1]. The paper presents results of 3D modelling using finite sized transducers to generate waves at an angle of incidence to a lap weld.

2 INVESTIGATION OF PROPAGATION OF SH AND S0 MODE PLATE WAVES IN UNCONSTRAINED TANK FLOOR WITH WELD BY 3D NUMERICAL MODELLING

2.1 DESCRIPTION OF 3D FINITE ELEMENT MODEL

The aim of the simulation is to investigate the properties of waves of different polarization propagating in structures made of several plates welded together. The lap welds as well as complex interaction of the plates with surrounding acoustic media (oil on one side and soil on another) makes the overall structure irregular. Practically, the only means to obtain realistic solutions is the finite element simulation by using 3D solid or coupled solid-acoustic models.

2.1.1 Geometry of the Model

The 3D finite element computational model composed of linear elastic elements has been built using ANSYS and LSDYNA finite element codes. ANSYS has been used to generate the volumes and to perform the meshing of the model. The problem is then solved in LSDYNA environment. The geometry of the model generated in ANSYS (APDL internal programming language) is fully parametric. Two models have been investigated:

- Two overlapping plates welded together, *Figure 1*;
- Three overlapping plates, *Figure 2*.

The parameters used for both sample calculations are presented in *Table 1*.

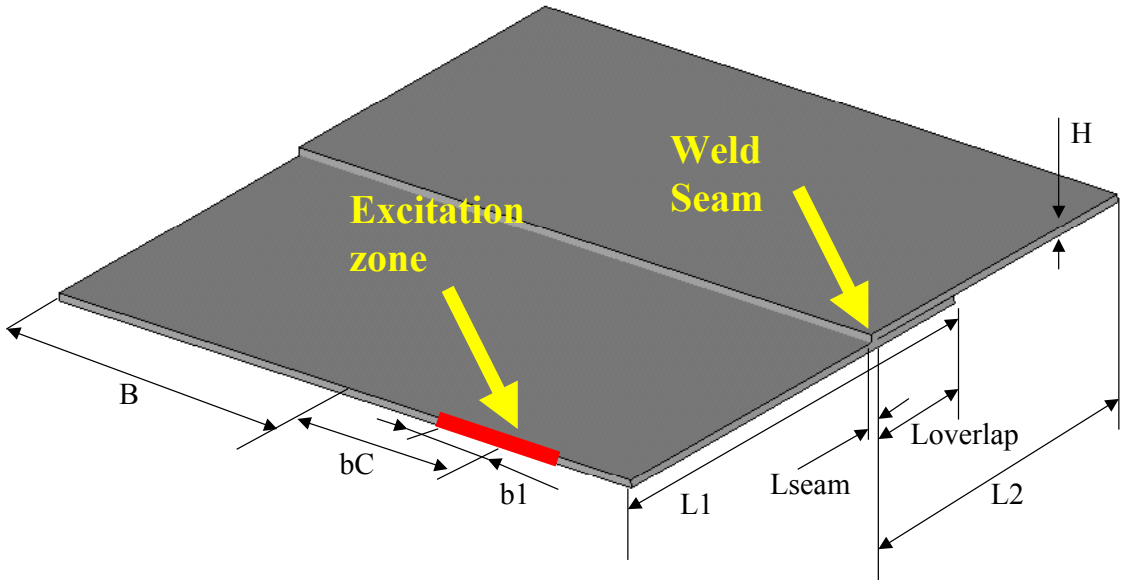

Figure 1. Two plates welded together: H is the plate thickness; B is the plate half-width; b_1 is the half-width of the excitation zone; b_C is the centre of the excitation zone; L_1 the 1st plate length; L_2 is the 2nd plate length; L_{seam} the width of the seam; $L_{overlap}$ the overlap length.

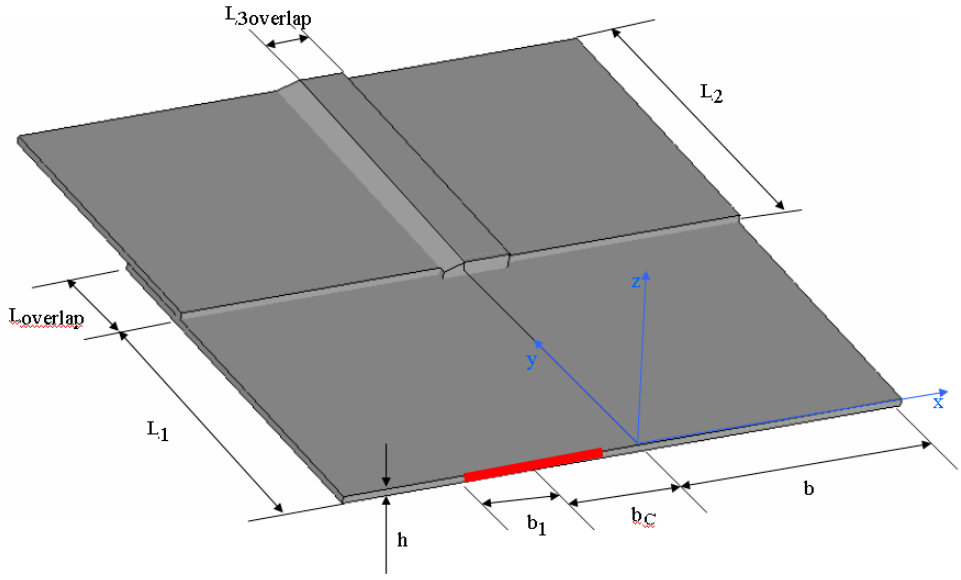

Figure 2. Three plates welded together: h is the plate thickness; b is the plate half-width; b_1 is the half-width of the excitation zone; b_C is the centre of the excitation zone; L_1 is the 1st plate length; L_2 is the 2nd plate length; L_{seam} the width of the seam; $L_{3overlap}$ is the overlap length of the two plates.

Table 1. The parameter values used in the calculation.

	H, [mm]	B, [mm]	b_1, [mm]	b_C, [mm]	L_1, [mm]	L_2, [mm]	L_{seam}, [mm]	$L_{overlap}$, [mm]
Two welded plates	6	250	50	0/-100	250	250	6	80
Three welded plates	6.17	249	24.7	24.7	249	249	6	39.1/80 (L3)

The size of an element is selected based on the consideration that 20-30 elements should be used per wavelength.

Element type 99 of LSDYNA program has been used in the model. The element is intended for vibration studies carried out in the time domain. These models may have very large numbers of elements and may be run for relatively long durations. The purpose of the element is to achieve substantial CPU savings. This is achieved by imposing strict limitations on the range of applicability, thereby simplifying the calculations:

- Elements must be cuboids; all edges parallel to the global x,y,z axes;
- Small displacement, small strain, negligible rigid body rotation;
- Elastic material only.

With this element, the performance of the model is similar to the fully integrated solid, however the performance is even better than that of traditional constant strain element. Single element bending and torsion modes are included, so meshing guidelines are as for fully integrated solids - e.g., thin structures can be modeled with a single solid element through the thickness if required.

In order to satisfy the requirements posed upon the element geometry, the welded seam has been modeled as a line of elements with a rectangular cross section. It appears reasonable to expect that the micro-geometry of the cross-section will not substantially influence the simulation results as the wavelengths investigated here are considerably (about 6-7 times) larger.

2.1.2 Material model

The whole assembly is assumed to be a homogeneous elastic steel structure and is modeled in LSDYNA by using *MAT_ELASTIC model as presented in *Table 2*.

Table 2. The parameters of *MAT_ELASTIC model, where ρ is mass density, E is Young's modulus, σ is Poisson's ratio.

$ STEEL elastic			
*MAT_ELASTIC			
$MID	ρ	E	σ
1	7800	2.0533E+11	0.29

From theses values, the longitudinal and transverse (shear) wave velocities are c_L=5900m/s, c_T=3190m/s. The shortest expected wavelength at 50kHz frequency excitation is 63.8mm and by taking 25 elements per wavelength we have an element size of 2.552mm. So for the 250x500x6mm plate we need 98x196x3=57624 elements or 78012 nodes. If local behavior of the wave near, say, defect edges is to be investigated where wave transformations and generation of higher frequency components may take place, a finer mesh would be required.

2.1.3 Boundary Conditions

The structure for ultrasonic wave propagation simulation is unsupported, as is the usual practice in modelling of problems of high-frequency vibration. The weld in the model (see L_{seam} in *Figure 1*) indicates the ideal connection (coincidence) of nodes. The overlapped region (see $L_{overlap}$ in *Figure 1*) of the two plates can also be treated as a free boundary. The reason is that the amplitudes of the investigated waves are small enough to avoid interaction between the plates because of the small gap which exists in reality between the plates in non-welded regions.

2.1.4 Wave Mode Excitation

The ultrasonic wave is excited by means of a piezoelectric transducer (PT). Due to the inverse piezoelectric effect phenomenon the PT deforms under the influence of an applied external electric field. The simplest approximation of the phenomenon may be presented by means of the equivalent force diagram,
Figure 3. The deformation excited in the PT is defined as

$$S_J = d_{iJ} E_i ,$$

where d_{iJ} is the piezoelectric strain modulus (i=1,2,3 correspond to the three longitudinal directions of possible application of an electric field E_i), S_J - the strain tensor presented in Voigt's notation (J=1,2,3 correspond to the three longitudinal components of the strain and J=4,5,6 - to shear strains in coordinate planes xy, xz, yz correspondingly). In approximate evaluations it is usually assumed that the deformation mode of the PT under the electric field E_i applied in direction i is determined by the largest value $\max_J d_{iJ}$. The stresses caused by the piezoelectric effect phenomena can be conveniently presented as $T_J = d_{iK} c_{KJ} E_i = e_{iJ} E_i$, where e_{iJ} is the piezoelectric coefficient $e_{iJ} = d_{iK} c_{KJ}$, and c_{KJ} is the stiffness tensor determined under constant electric field. The scheme of stresses in the plate created by means of its interaction with the PT excited by the electric field component E_1 is presented in *Figure 3*. The excitation waveform is a 50kHz sinusoidal tone burst.

2.1.5 Exciting Waves Propagating at an Angle to the Boundary

The transducers shown in *Figure 3* are divided into sub elements. If these are driven uniformly, waves propagating in the direction normal to the boundary of the plate are generated. The transducer elements can be driven with phase delays to generate waves at an angle.

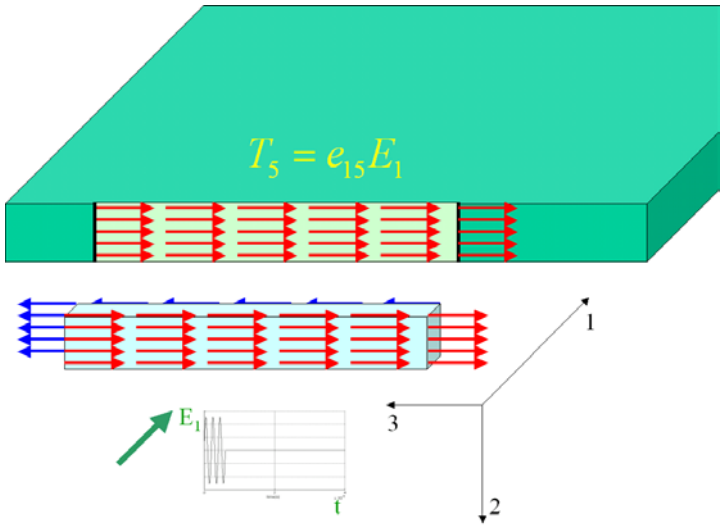

a)

(continued on next page)

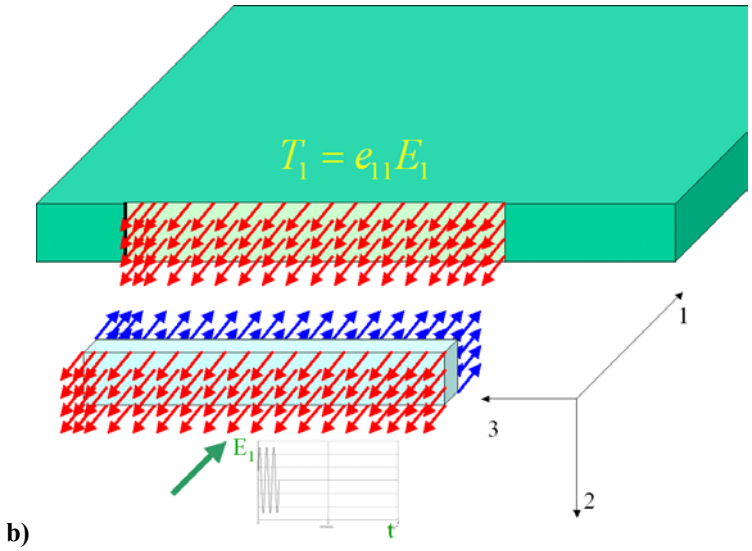

Figure 3. Free body diagram of the excitation of shear (a) and longitudinal (b) ultrasonic waves. Shear (a) or longitudinal (b) stress components are excited in the piezoelectric transducer as a consequence of the electric field component E_1 and causes the corresponding interaction stress to be created in the plate.

2.2 PROPAGATION OF S_H AND S_0 MODE WAVES IN UNCONSTRAINED DAMAGED FLOOR

The propagation of the S_0 mode Lamb waves has been investigated in previous stages of the project. The investigation of the interaction of these waves with the lap joint weld has been also performed using 2D models [1]. The objective at the present stage of modelling was to investigate the features of the S_0 and S_H plate waves interaction with the weld and defect in 3D. *Figure 4* to *Figure 7* present the distribution of acoustic field in the welded or defected plate at different time instances with different excitation conditions. In these figures the amplitude of the particle velocity vector is denoted by the colour coding. The vertical particle displacement can be observed as "surface wave" in 3D images. *Figure 4* presents the interaction of S_0 mode Lamb wave with the lap weld. It can be seen that after the interaction with the weld, the S_0 mode is partially reflected, transmitted and mode converted. A_0 Lamb wave are generated in the forward and backward directions. *Figure 5* also shows the case when the S_0 mode Lamb wave was generated at an angle with respect to the weld. The waves after the interaction have a similar character, but the A_0 Lamb is generated at an angle to the weld.

The propagation of the S_H waves is more complicated. Due to the finite dimensions of the transmitter some S_0 waves are generated from the transducer edges in addition to the pure S_H mode (*Figure 6a*). S_0 mode Lamb waves are faster then S_H mode Lamb waves, so they hit the weld first (*Figure 6b*) and generate A_0 Lamb waves. Later the slower S_H wave reaches the weld and generates additional A_0 waves (*Figure 6c*). It can also be observed that the amplitude of these secondary A_0 Lamb waves is less in the central part. Possibly, generation of the mode converted A_0 Lamb waves from the S_H mode waves is stronger when they hit the weld at an angle.

Figure 7 shows the interaction of the S_0 and S_H mode waves with a disk shape defect. The defect diameter is 50mm and it extends through half the plate thickness. It can be

seen that in both cases the defect is the source of A_0 Lamb waves which propagate almost uniformly in all directions. The particle displacement and particle velocity in the defect region have much higher amplitude, so it can be assumed that the defect acts as a virtual transmitter. If the plate is covered by some liquid medium, this virtual transmitter (defect) should generate acoustic waves propagating into the liquid. The directivity of this generation of course depends on the defect geometry. It can be observed that the S_0 Lamb wave propagates through the defect almost without decay, while the S_H mode has some amplitude decay in the region after the defect. This can be explained by the fact that the wavelength of S_0 mode is almost twice the diameter of the defect, while the S_H wavelength is comparable with the size of the defect. So, the S_0 Lamb wave is diffracted around the defect and decay of the amplitude can not be observed.

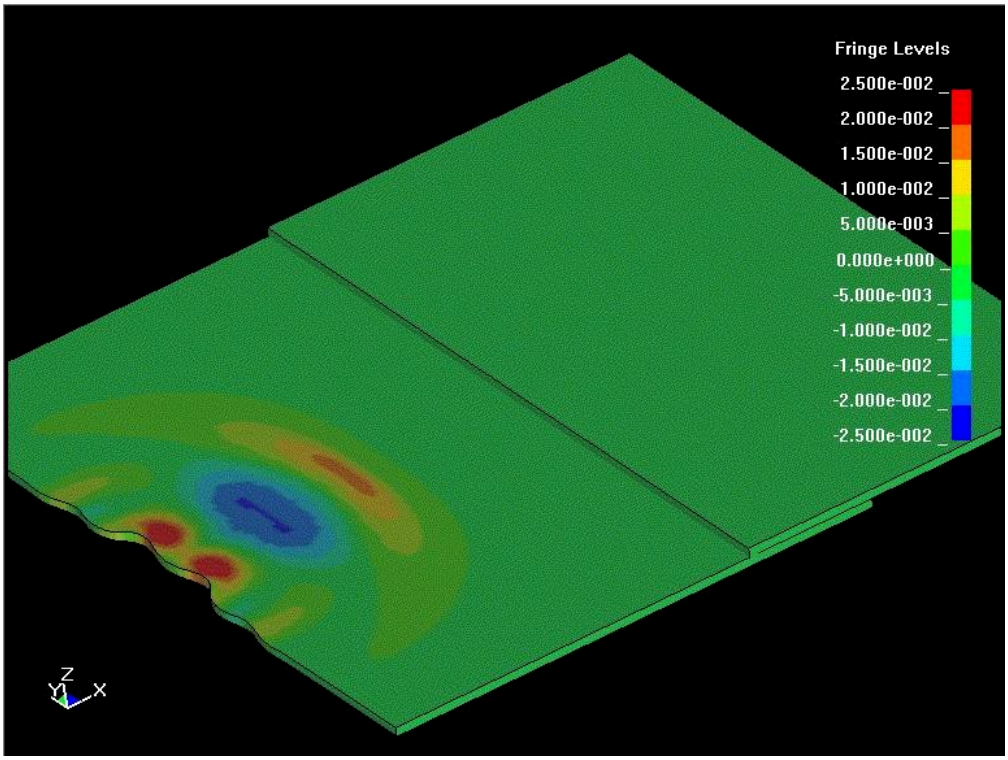

a)

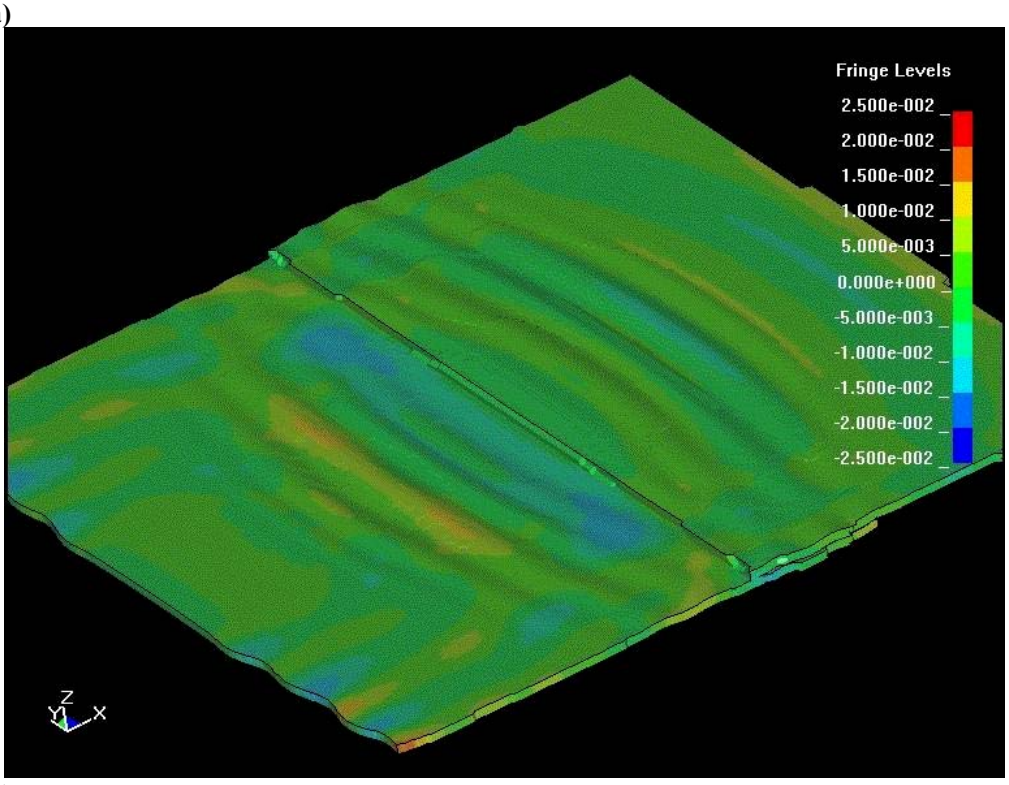

b)

Figure 4. Acoustic field of S_0 Lamb wave before hitting the lap joint weld (a) and after interaction with weld (b).

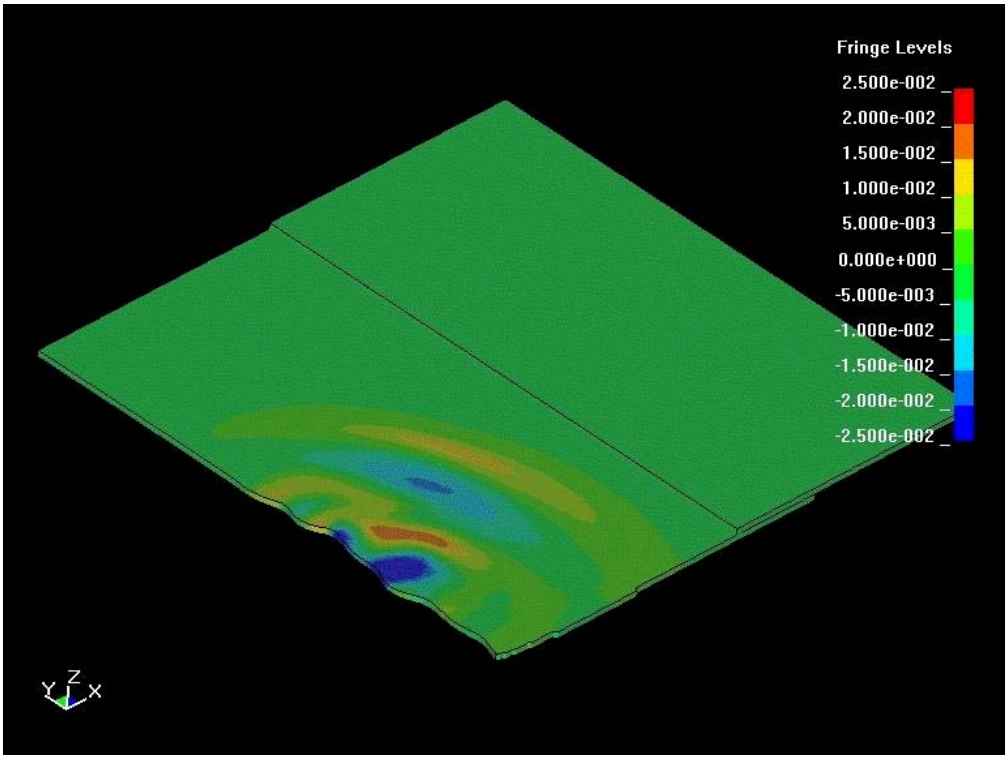

a)

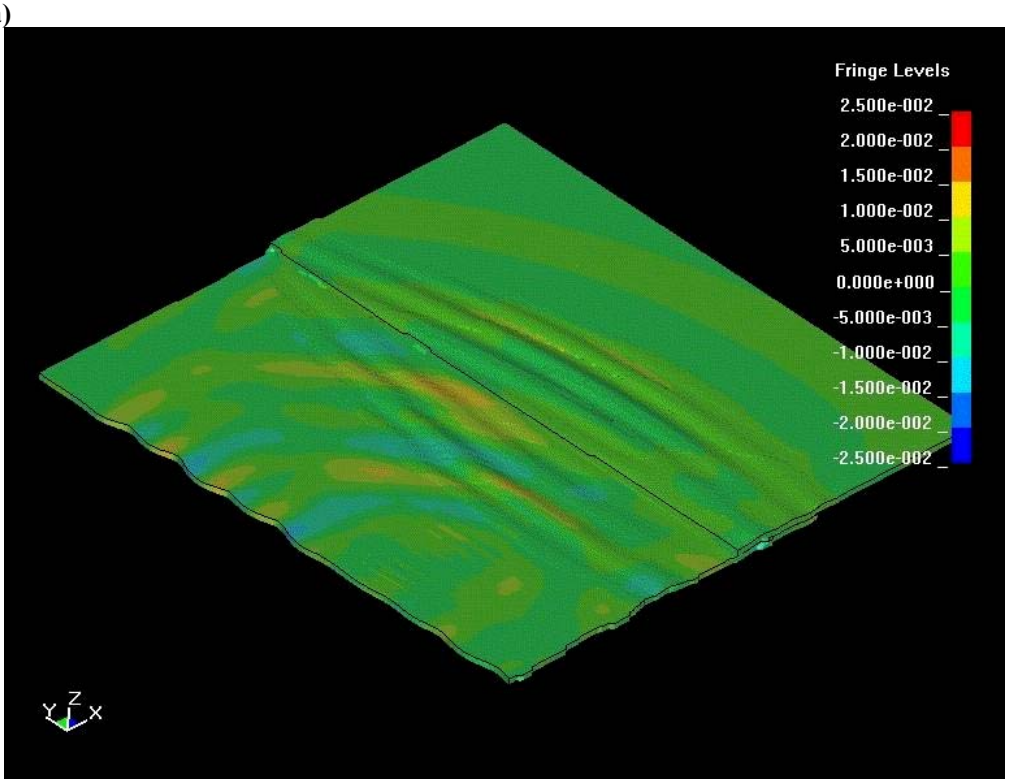

b)

Figure 5. Acoustic field of S_0 Lamb wave before hitting the lap joint weld (a) and after interaction with weld (b). The waves are generated at 30° with respect to the weld.

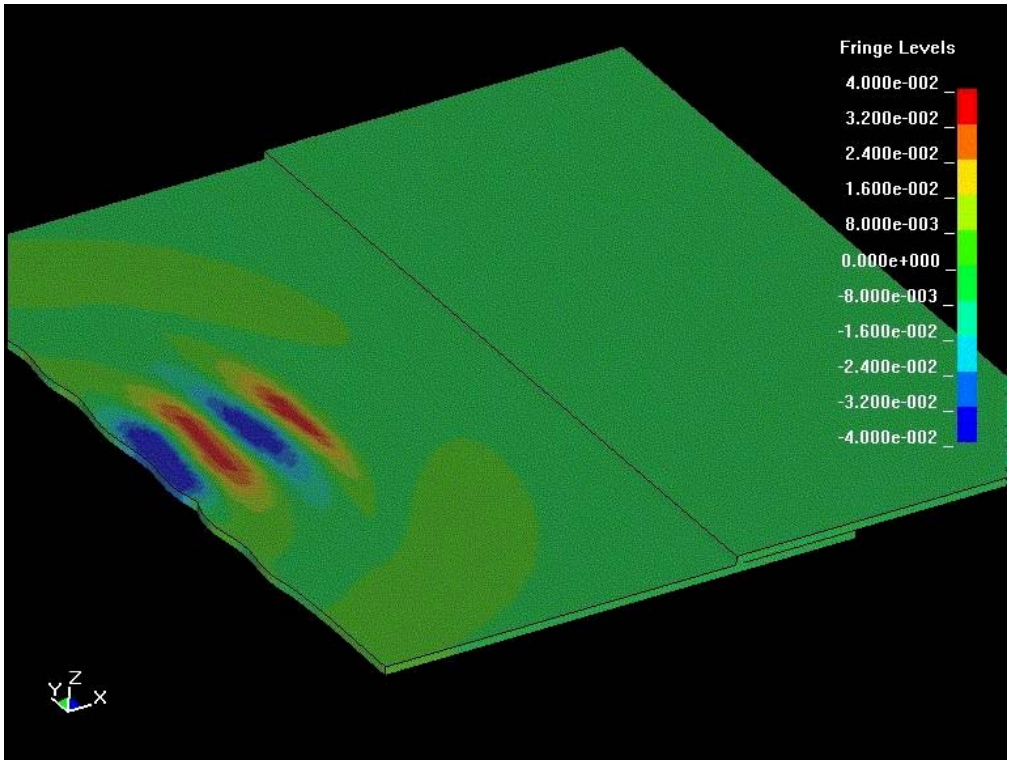

a)

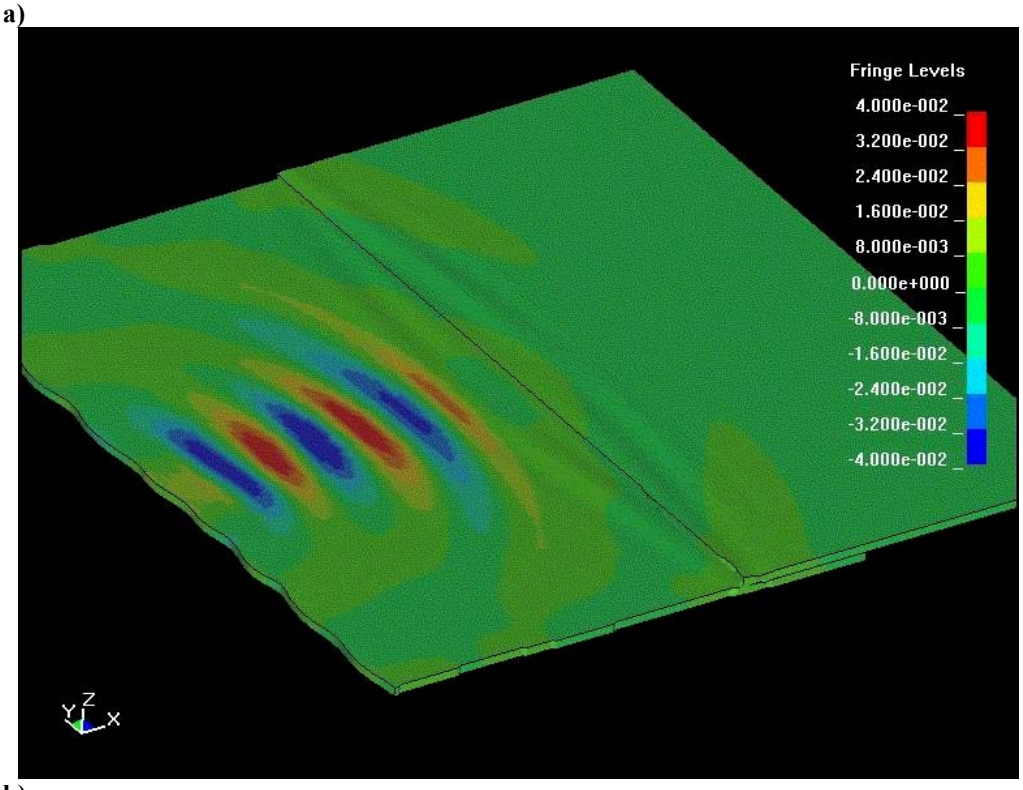

b)

(Continuation on next page)

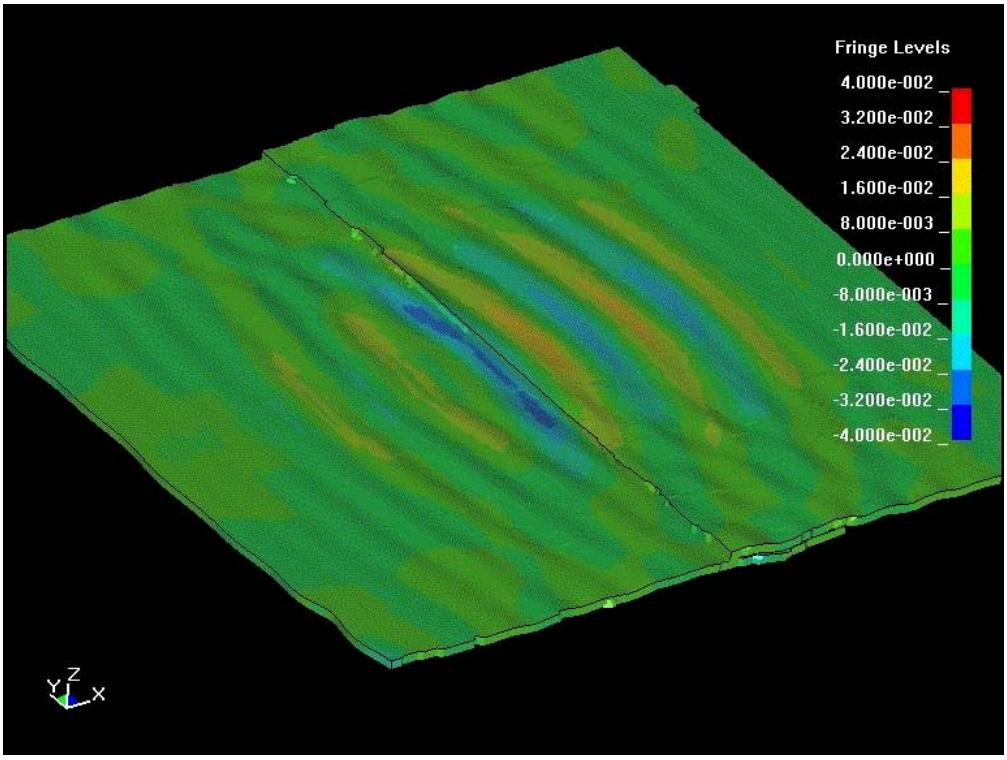

c)

Figure 6. Acoustic field of S_H wave before hitting the lap joint weld (a), at the instant when S_0 Lamb wave hits the weld (b) and after interaction with weld (c).

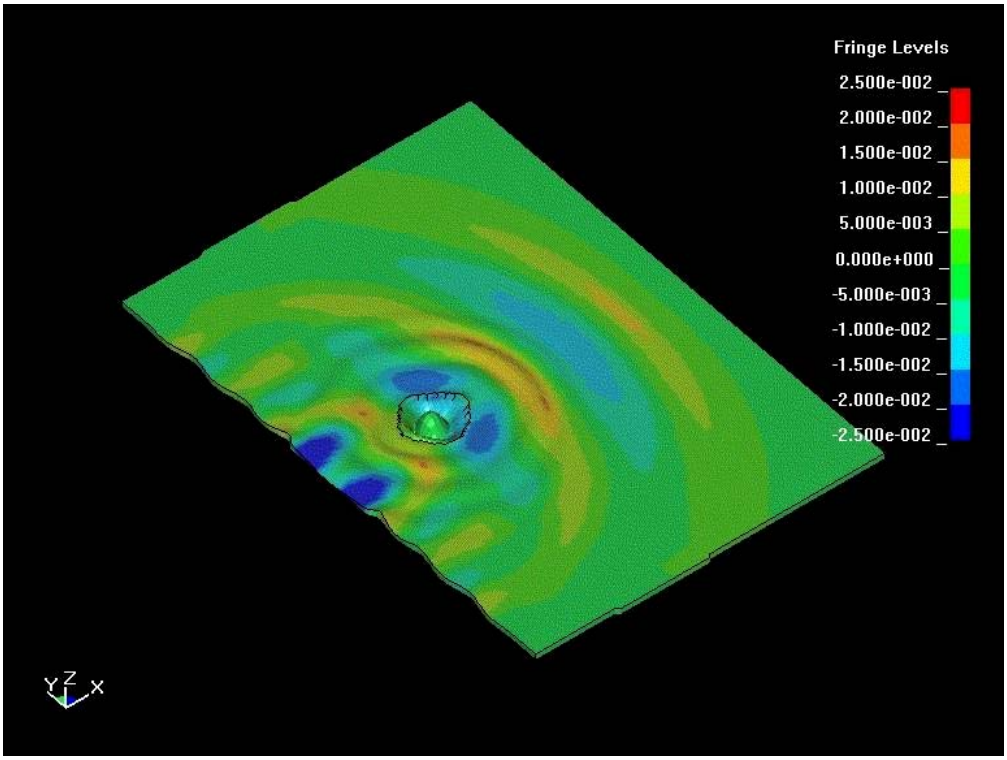

a)

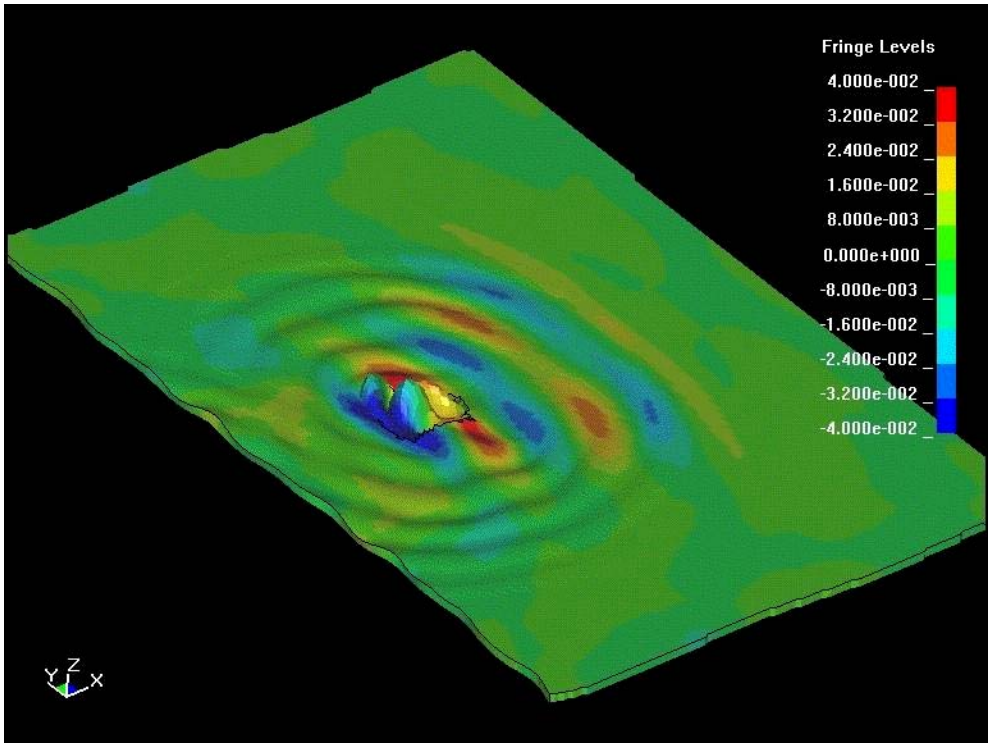

b)

Figure 7. Interaction of the S_0 (a) and S_H (b) waves with the disk shaped defect, 50mm diameter (0.5 wall thickness).

2.3 PROPAGATION OF S_H AND S_0 MODES IN 3D LAP JOINTS

The interaction of the S_0 mode Lamb wave with the 3D lap joint is shown in *Figure 8* to *Figure 9*. In all cases the waves were generated at 30° with respect to the normal of the plate edge. *Figure 8* shows the distribution of *y* component of particle velocity before and after hitting of the weld by the S_0 mode wave. The essential decay of the wave amplitude can be observed after the joint. The results presented in *Figure 9* demonstrate that due to the interaction the A_0 mode Lamb wave is generated. In *Figure 10* to *Figure 11* similar results obtained with the S_H mode wave are presented. Comparison between the S_0 and S_H mode waves demonstrates that the S_H mode passes the lap joint with lower attenuation that the S_0 mode. It can be seen also that that the amplitude of the secondary A_0 wave is smaller than for the S_H mode wave. For more detailed estimation of the wave attenuation caused by the weld, the waveforms of corresponding *y* and *x* components of particle velocity were acquired at the points shown in *Figure 12*. Comparison of amplitudes of the waveforms before the weld (point P_1) and after (point P_2) have shown that the attenuation of the S_0 mode is approximately 7dB and that of the S_H mode wave is about 11dB. This estimation (attenuation of the S_H mode > S_0 mode) contradicts the conclusions made from the 3D images. This can be explained by the fact that the point based estimations depend on the selected point, because the field is very non-uniform due to interference of different reflections. Nevertheless, the obtained value in general coincides with the results of 2D modelling and experimental investigations presented previously [1]

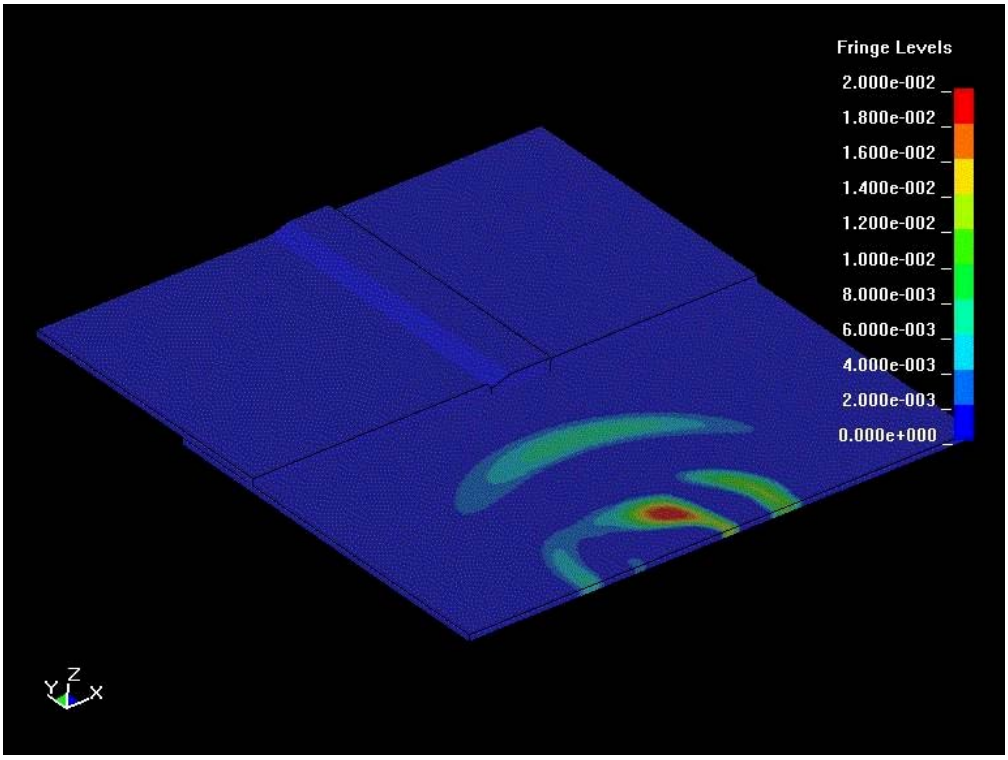

a)

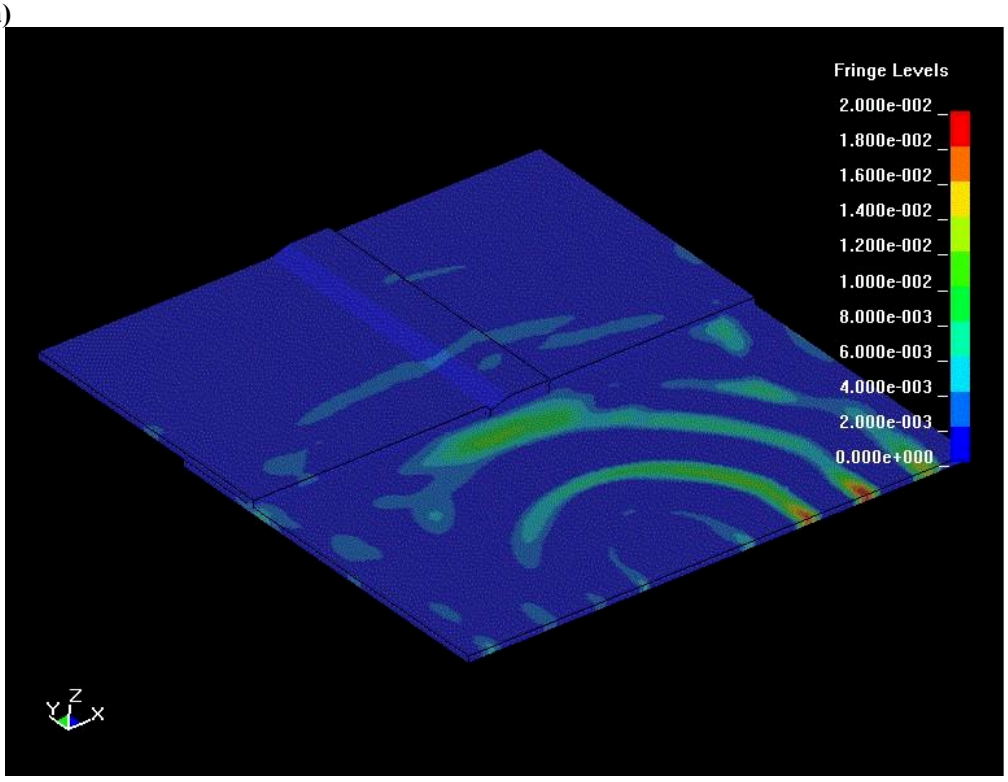

b)

Figure 8. Distribution of the y component of the particle velocity of S_0 Lamb wave before hitting the 3D lap joint weld (a) and after interaction with the weld (b).

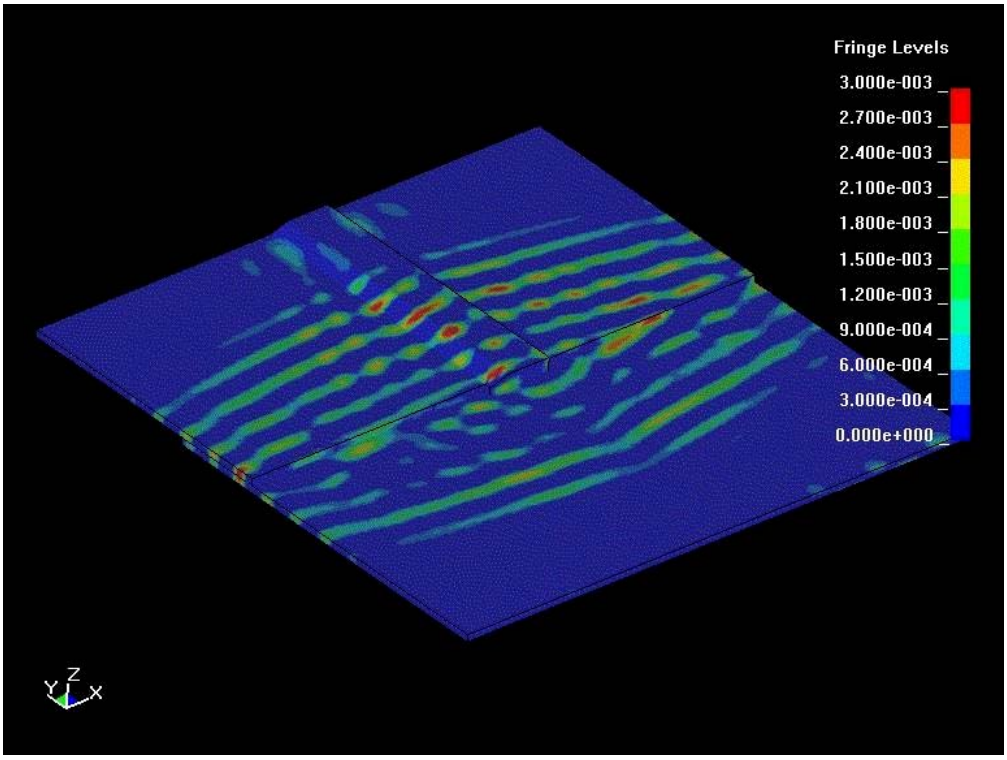

Figure 9. Distribution of the z (normal) component of the particle velocity of S_0 Lamb wave after interaction with the weld.

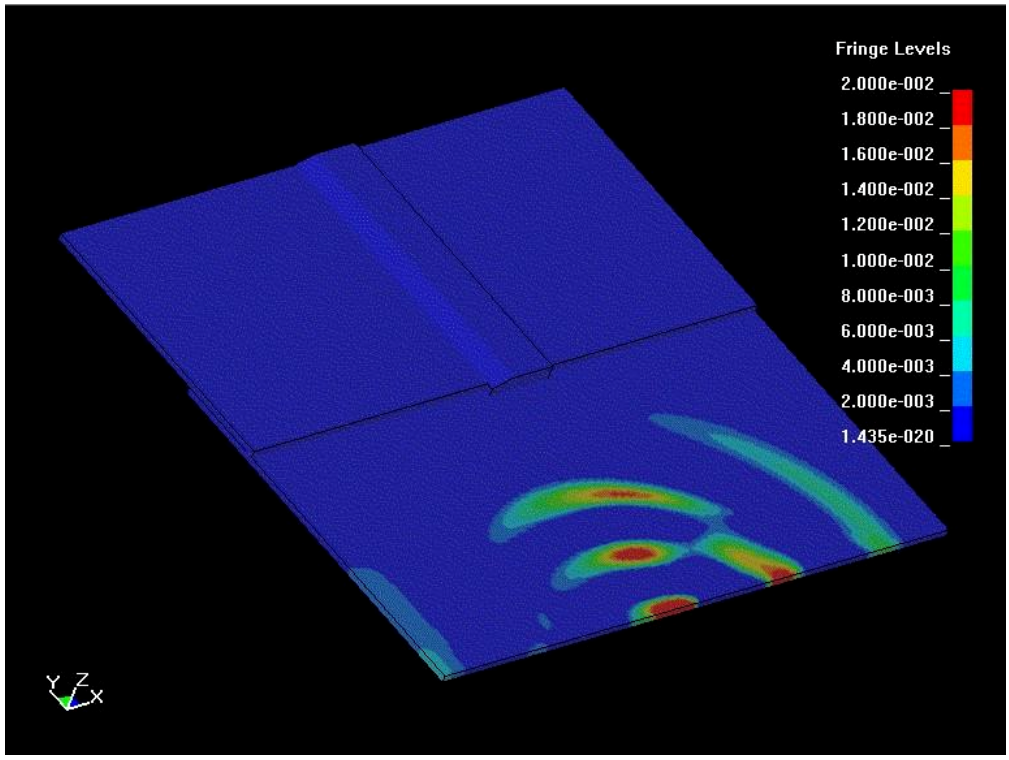

a)

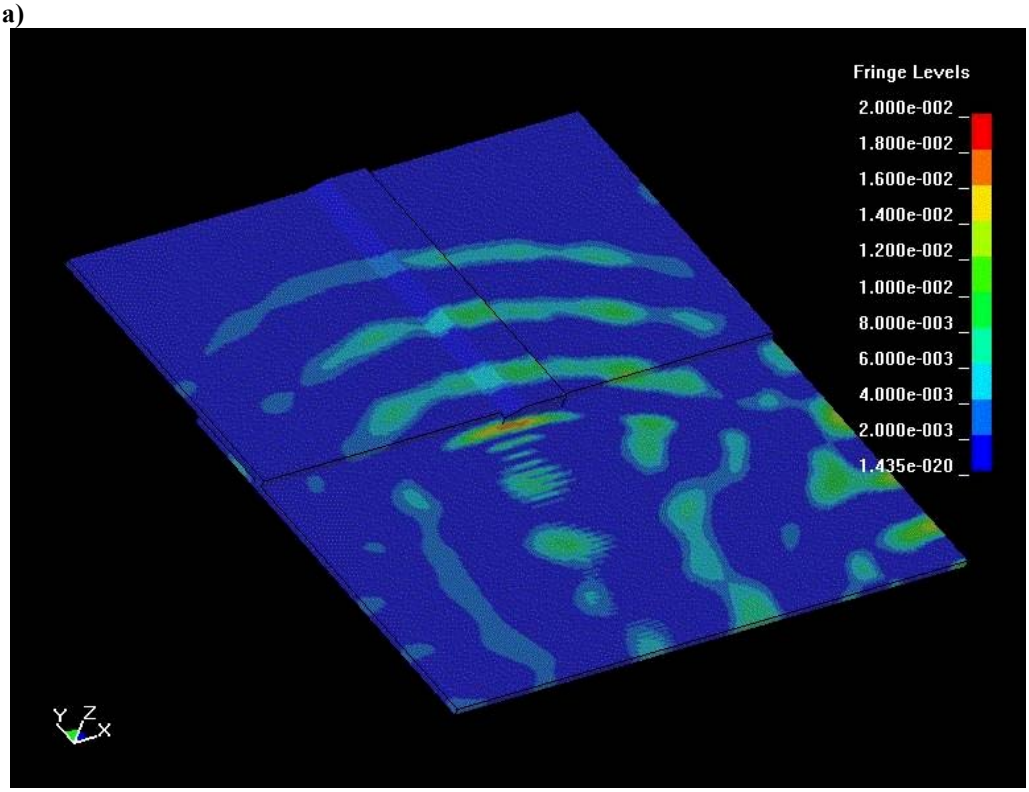

b)

Figure 10. Distribution of the x component of the particle velocity of S_H wave before hitting the 3D lap joint weld (a) and after interaction with the weld (b).

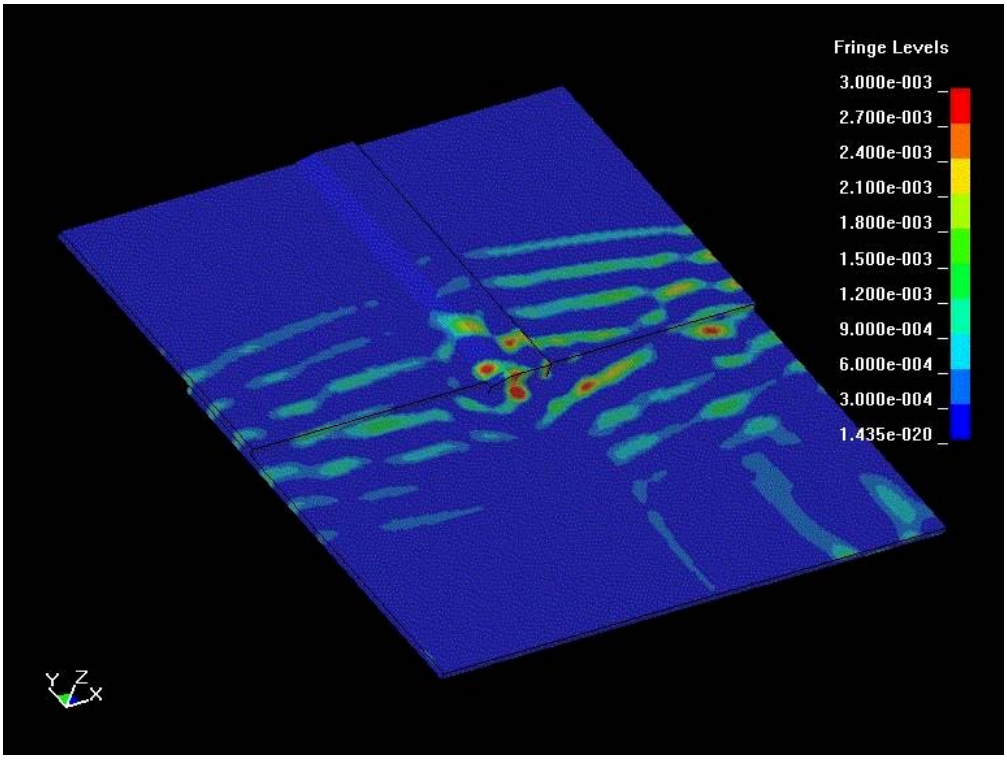

Figure 11. The distribution of the z (normal) component of the particle velocity of S_H mode Lamb wave after interaction with the weld.

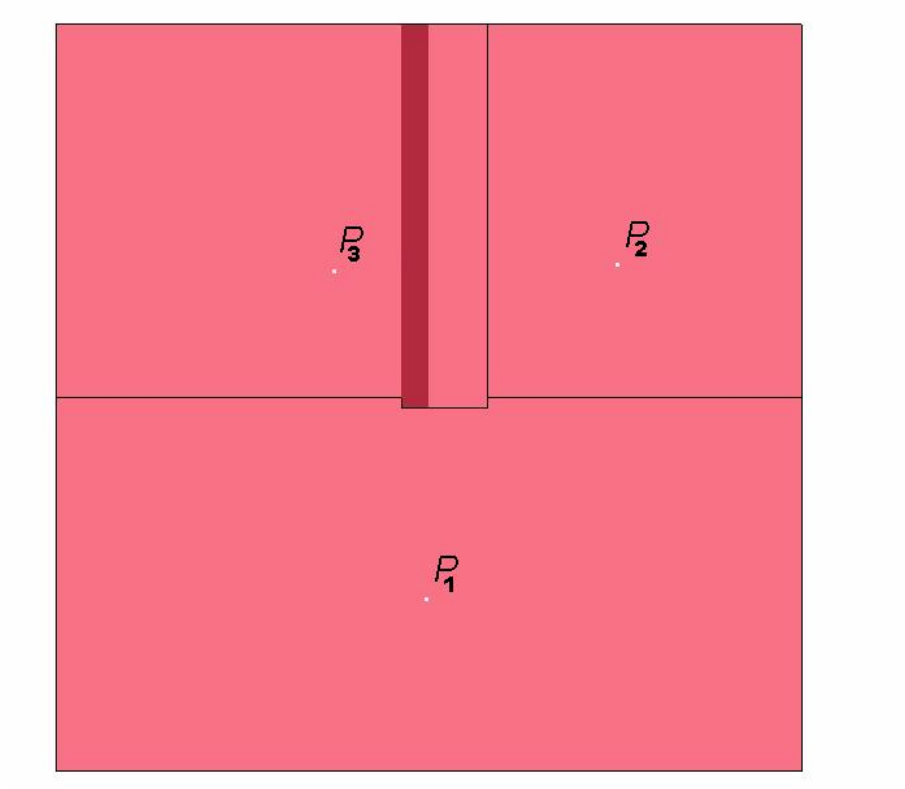

Figure 12. The points in the 3D model at which the waveforms were acquired for estimation of attenuation.

2.4 Experimental Results

Experiments have been carried out with a linear array of shear transducers dry coupled to the edge of a steel plate. Propagation distances of over 100 metres have been achieved.

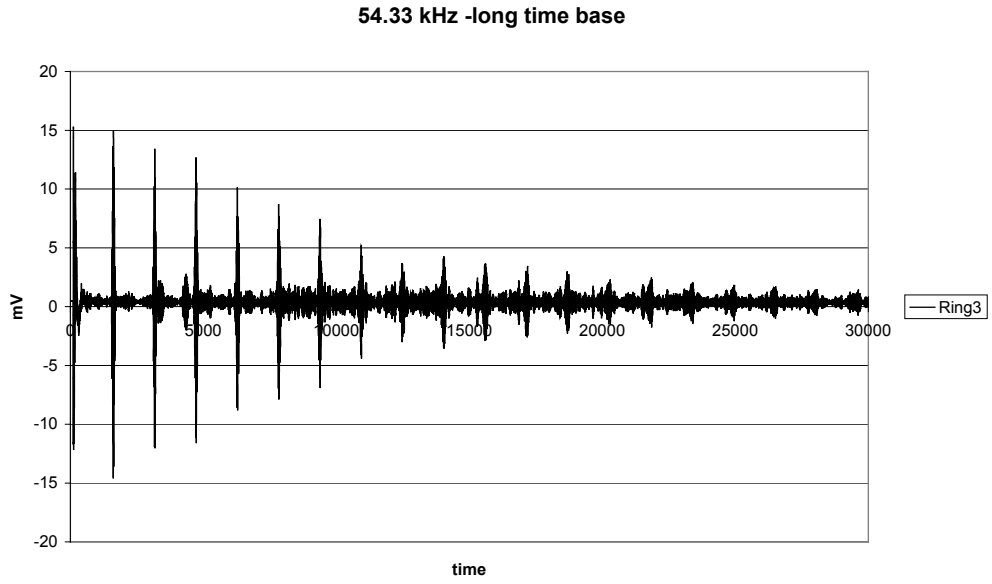

Figure 13. Experimental result showing 54.33 kHz S_H waves propagating in a 2.5m long steel plate.

3 CONCLUSION

Both theoretical modelling and experiments indicate that Long Rang ultrasound can be used to inspect the bottom plates of storage tanks.

4 REFERENCES

1, R.Kazys, L.Mazeika, A. Demcenka ,V. Cicenas and Ruth Sanderson, “Condition monitoring of large oil and chemical storage tanks using guided waves” Insight 2004